

Supporting Information for

Mixed-component sulfone–sulfoxide functionalized zinc IRMOFs: *in situ* ligand oxidation, carbon dioxide and water sorption studies.

Macguire R. Bryant[†], Andrew D. Burrows[‡], Cameron J. Kepert[§], Peter D. Southon[§], Omid T. Qazvini[¶], Shane G. Telfer[¶], and Christopher Richardson^{†*}

[†]School of Chemistry, University of Wollongong, Northfields Avenue, Wollongong NSW 2522, Australia

[‡]Department of Chemistry, University of Bath, Claverton Down, Bath BA2 7AY, United Kingdom

[§] School of Chemistry, University of Sydney, Sydney NSW 2006, Australia

[¶]MacDiarmid Institute for Advanced Materials and Nanotechnology, Institute of Fundamental Sciences, Massey University, Palmerston North, New Zealand

Contents

1. NMR spectra of Me ₂ bpdc-CH ₂ SO ₂ CH ₂ CH ₂ CH ₃ and H ₂ L ⁴	2
2. SCXRD of MSO ₂ Pr-100 (WUF-10)	4
3. Thermogravimetric–Differential Thermal Analyses.....	8
4. Gas Adsorption Analyses.....	11
5. Analyses Post Water Vapor Sorption	19
6. Multi-Point Brunauer–Emmett–Teller Analyses	20
7. Fitting Parameters for IAST calculations	21

1. NMR spectra of $\text{Me}_2\text{bpdc}-\text{CH}_2\text{SO}_2\text{CH}_2\text{CH}_2\text{CH}_3$ and H_2L^4

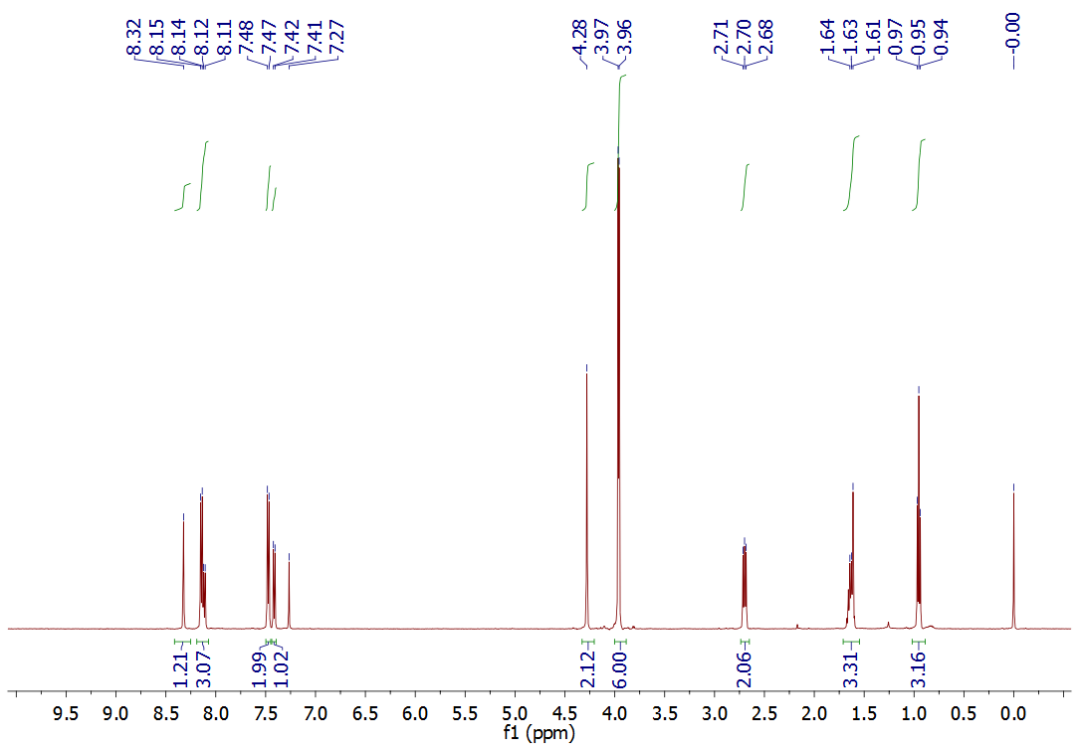


Figure S 1: ^1H NMR spectrum of dimethyl 2-((propylsulfonyl)methyl)-[1,1'-biphenyl]-4,4'-dicarboxylate, $\text{Me}_2\text{bpdc}-\text{CH}_2\text{SO}_2\text{CH}_2\text{CH}_2\text{CH}_3$

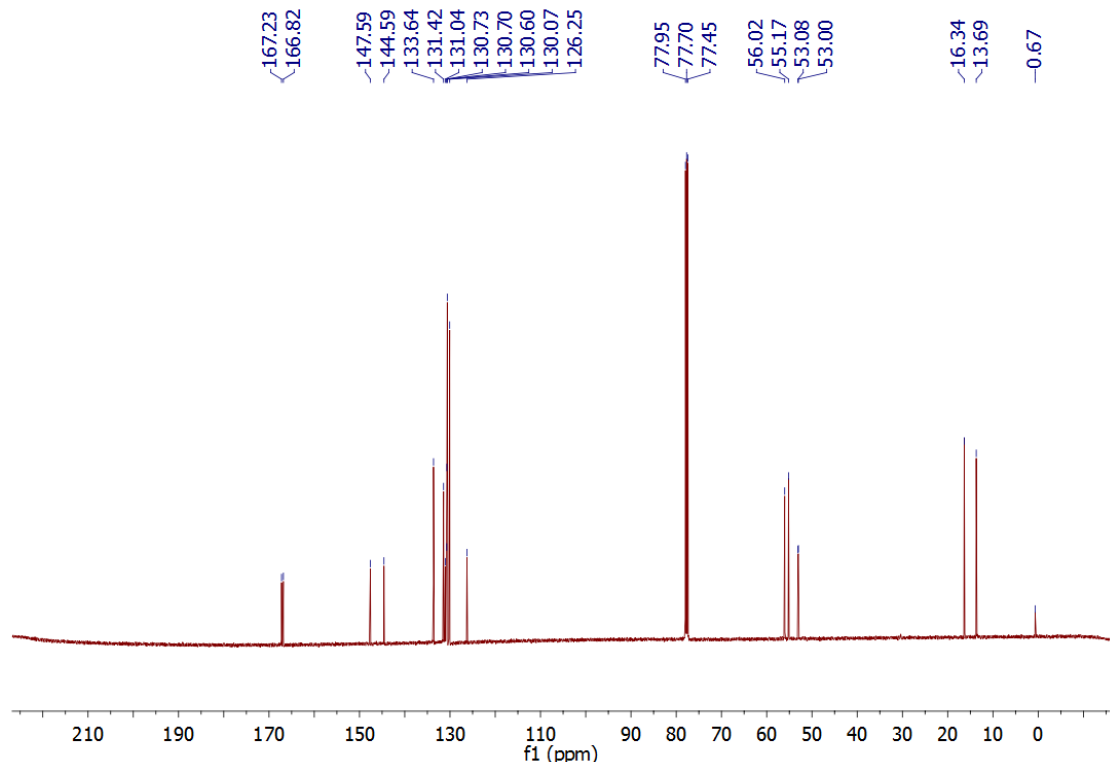


Figure S 2: ^{13}C NMR spectrum of dimethyl 2-((propylsulfonyl)methyl)-[1,1'-biphenyl]-4,4'-dicarboxylate, $\text{Me}_2\text{bpdc}-\text{CH}_2\text{SO}_2\text{CH}_2\text{CH}_2\text{CH}_3$

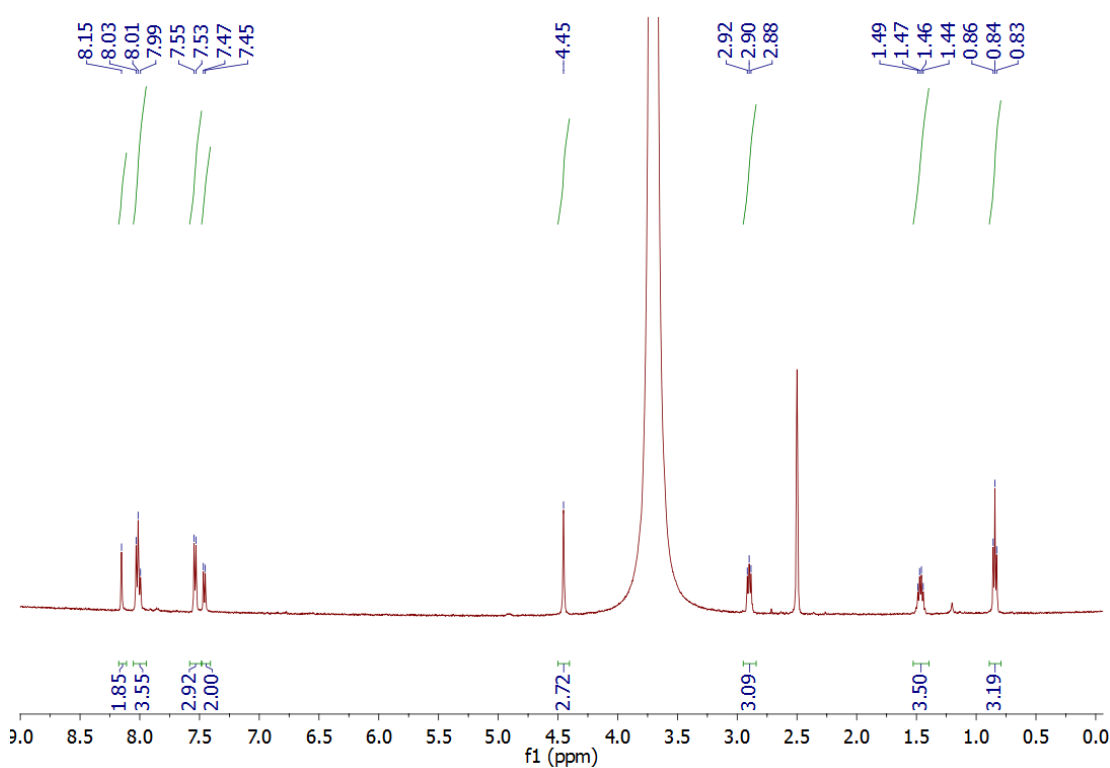


Figure S 3: ^1H NMR spectrum of 2-((propylsulfonyl)methyl)-[1,1'-biphenyl]-4,4'-dicarboxylic acid (H_2L^4)

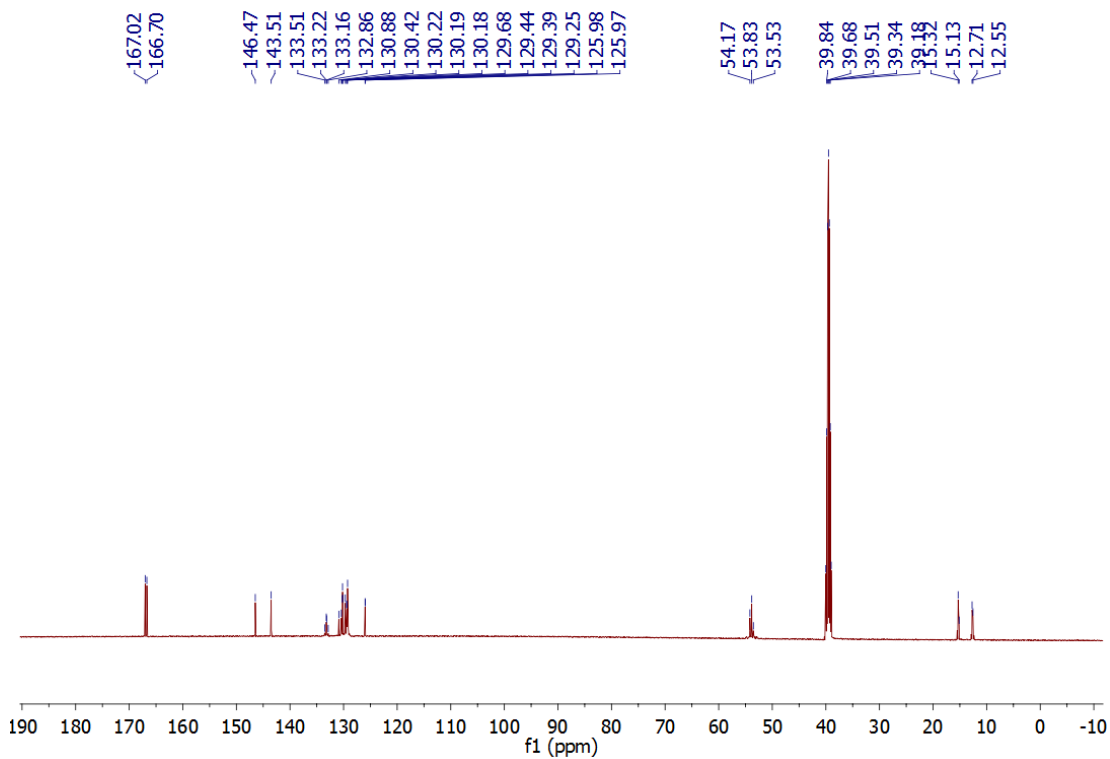


Figure S 4: ^{13}C NMR spectrum of 2-((propylsulfonyl)methyl)-[1,1'-biphenyl]-4,4'-dicarboxylic acid (H_2L^4)

2. SCXRD of $\text{MSO}_2\text{Pr-100}$ (WUF-10)

Table 1 Crystal data and structure refinement for WUF-10.	
Identification codes	WUF-10, CCDC 1503491
Empirical formula ^a	$\text{C}_{21}\text{H}_{13}\text{O}_7\text{Zn}_2$
Formula weight	508.05
Temperature/K	292
Crystal system	monoclinic
Space group	C2/m
$a/\text{\AA}$	24.6493(15)
$b/\text{\AA}$	24.0029(12)
$c/\text{\AA}$	17.2267(12)
$\alpha/^\circ$	90
$\beta/^\circ$	91.311(6)
$\gamma/^\circ$	90
Volume/ \AA^3	10189.6(11)
Z	8
$\rho_{\text{calc}}/\text{cm}^3$	0.662
μ/mm^{-1}	1.304
F(000)	2040.0
Crystal size/mm ³	0.15 × 0.10 × 0.05
Radiation	$\text{CuK}\alpha (\lambda = 1.54178)$
Resolution range for data/ \AA	8.0 – 1.37
Index ranges	-17 ≤ h ≤ 17, -17 ≤ k ≤ 17, -12 ≤ l ≤ 12
Reflections collected	18884
Independent reflections	2165 [$R_{\text{int}} = 0.1609$, $R_{\text{sigma}} = 0.1728$]
Data/restraints/parameters	2165/82/161
Goodness-of-fit on F^2	2.930
Final R indexes [$I \geq 2\sigma(I)$]	$R_1 = 0.1853$, $wR_2 = 0.4482$
Final R indexes [all data]	$R_1 = 0.2174$, $wR_2 = 0.4648$
Largest diff. peak/hole / e \AA^{-3}	1.46/-0.72

^a The sulfone side-chain was not modelled.

Data on WUF-10 were collected at room temperature using a high-intensity rotating anode source. Despite this, reflections at high angles could not be observed owing to the limited crystallinity of WUF-10. This is a common observation for metal-organic frameworks. No diffraction could be observed at low temperatures.

The diffraction data lead to an overall structure of the Zn_4O SBU and the ligand backbone that is clear, chemically reasonable and in accord with related IRMOFs. In this sense the analysis has served the purpose of unambiguously determining the topology and interpenetrated structure of the metal-organic framework, which was the goal of the diffraction experiment. The limited quality of the diffraction data hampered free refinement

of the model. In order to build sensible phenyl rings of the ligands, and to allow a stable refinement, these atoms were subject to numerous distance restraints and were kept isotropic. The atoms of the sulfone-containing tag group were not found in the Fourier map, however, this is commonly observed for pendant groups with conformational freedom and disorder. As a result these atoms were not included in the model. It should also be noted that the data have not been subjected to the SQUEEZE procedure.

The asymmetric unit in this structure comprises one full zinc atom (Zn2) and one complete L^4 ligand moiety (O20 to O37). Also in the asymmetric unit are the zinc atoms Zn1 and Zn3, oxygen atom O4 (the μ_4 -oxygen in the centre of the SBU), an aqua ligand (O2) coordinated to Zn3 and another L^4 ligand (O5 to O19) (Figure S5). Atoms Zn1, Zn3, O2, O4, O5, O6, C7-C14, C17 and C18 lie on a mirror plane intrinsic to the space-group symmetry. Zn1 and Zn2 have tetrahedral coordination geometries and Zn3 is 5 coordinate trigonal bipyramidal due to the coordination of the aqua ligand. Large channels exist in the structure running parallel to the c axis as shown in Figure S8.

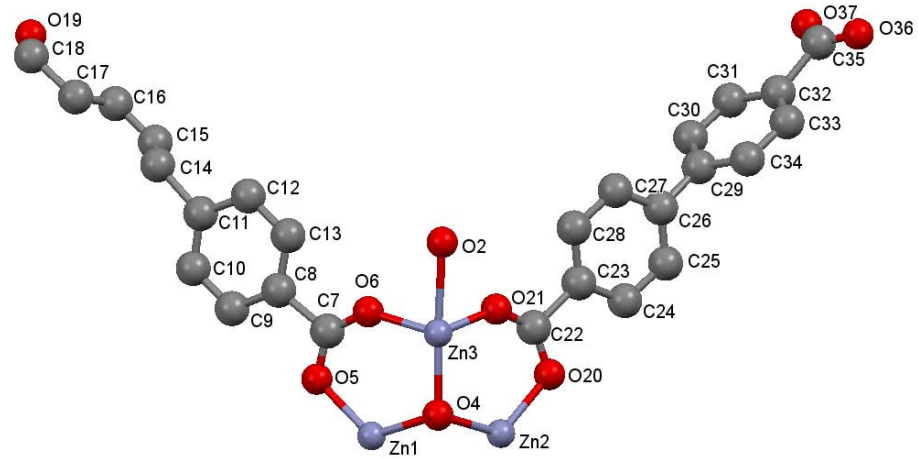


Figure S 5: Asymmetric unit of $\text{MSO}_2\text{Pr}-100$

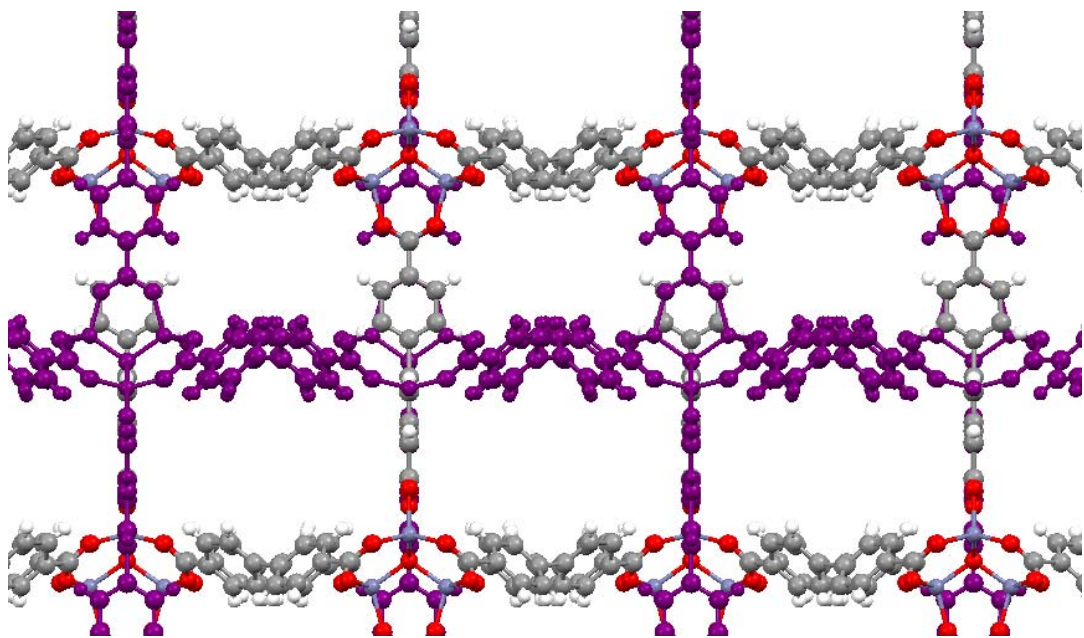


Figure S 6: A view of the crystal structure of $\text{MSO}_2\text{Pr-100}$ as viewed parallel to the crystallographic a axis. Interpenetrating framework coloured purple for clarity.

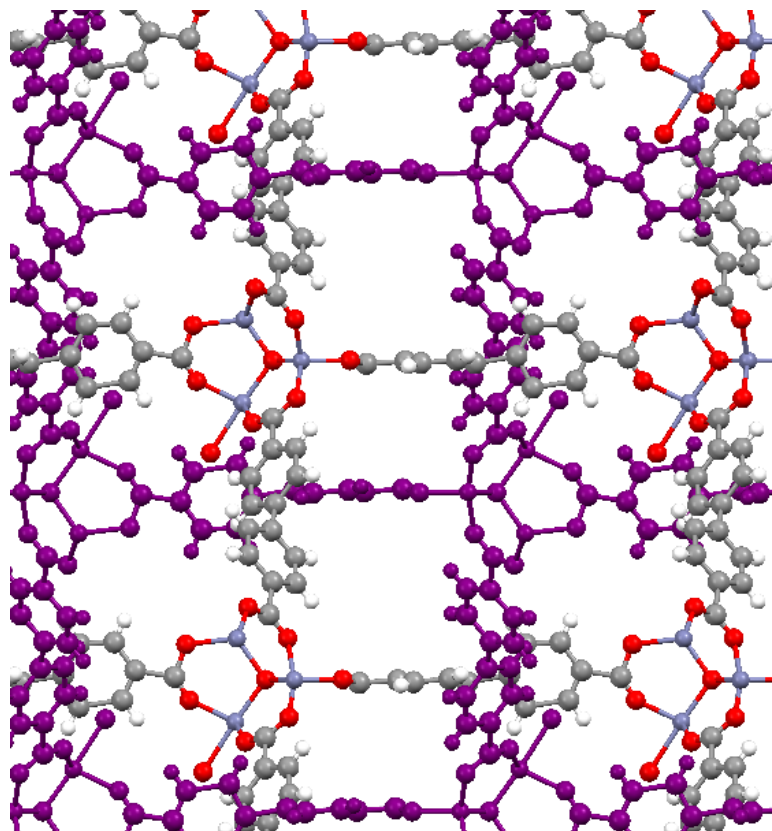


Figure S 7: A view of the crystal structure of $\text{MSO}_2\text{Pr-100}$ as viewed parallel to the crystallographic b axis. Interpenetrating framework coloured purple for clarity.

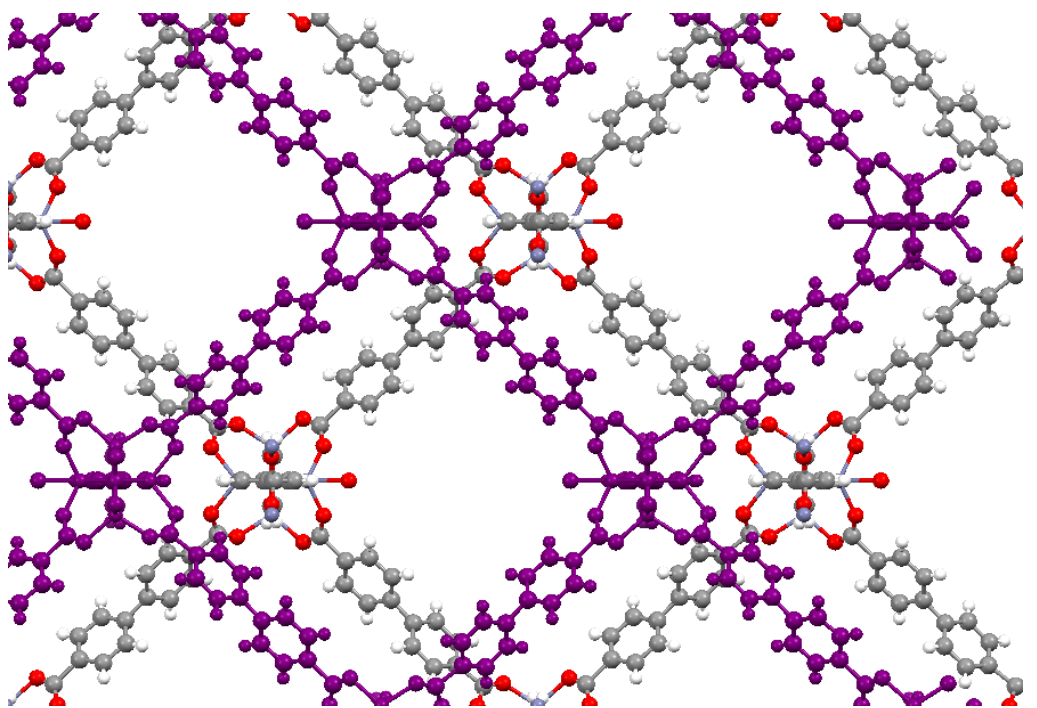


Figure S 8: A view of the crystal structure of $\text{MSO}_2\text{Pr}-100$ parallel to the crystallographic c axis. Interpenetrating framework coloured purple for clarity.

3. Thermogravimetric–Differential Thermal Analyses

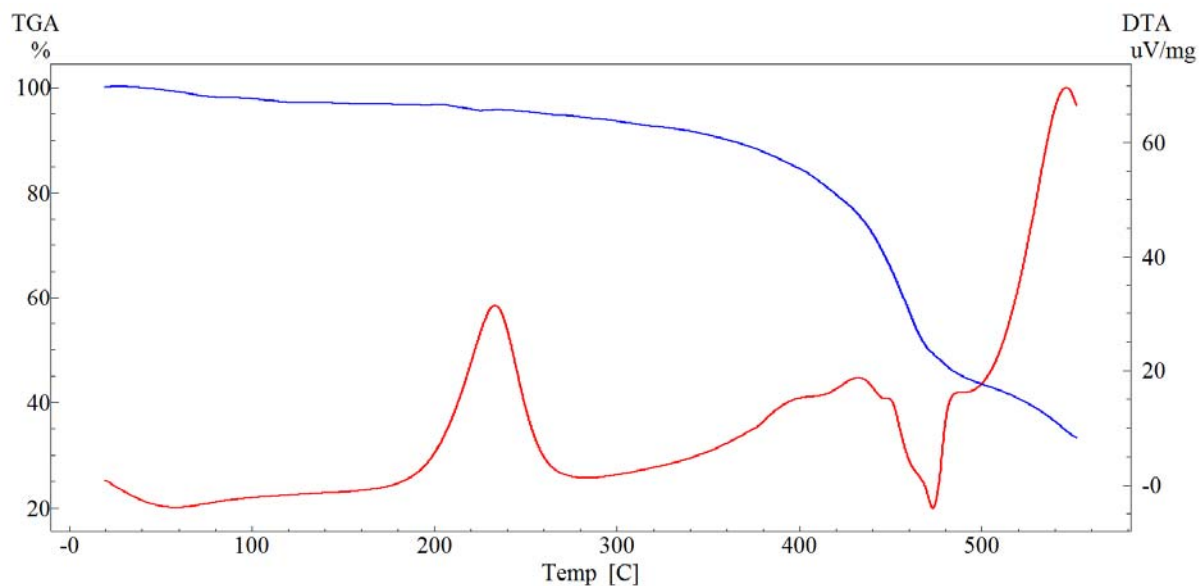


Figure S 9 : TG-DTA of MSO₂Me-15. Red trace (DTA response), blue trace (mass response).

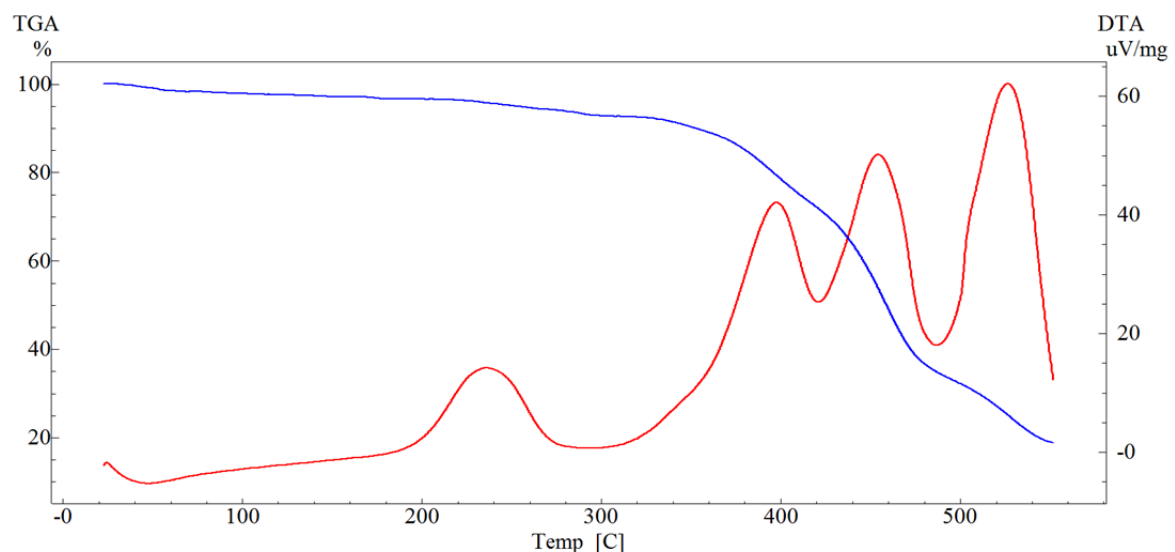


Figure S 10: TG-DTA of MSO₂Me-36. Red trace (DTA response), blue trace (mass response).

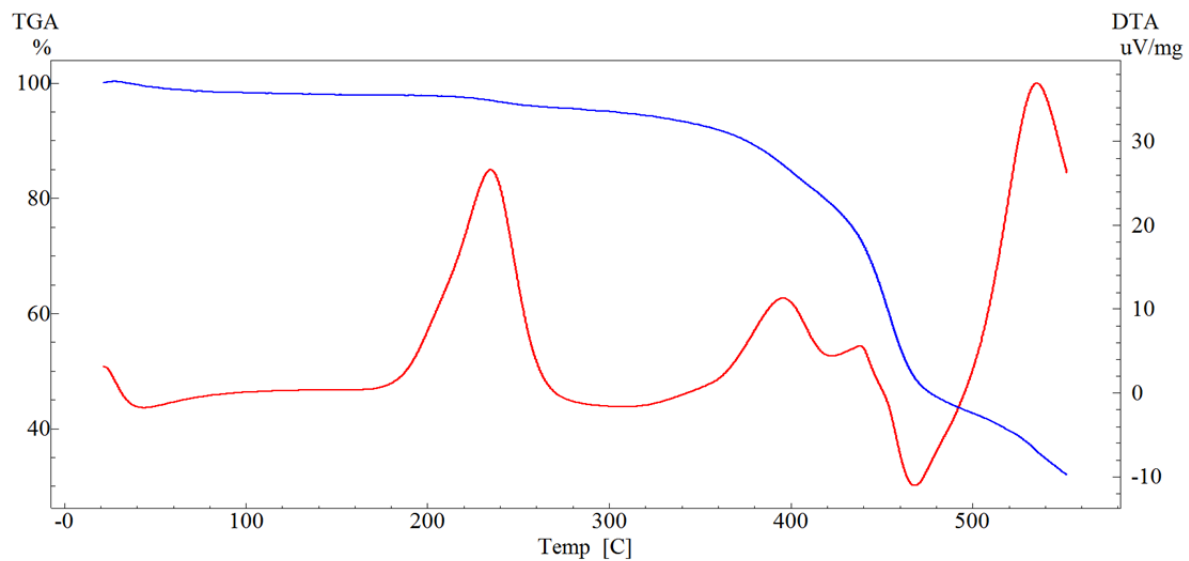


Figure S 11: TG-DTA of MSO₂Me-64. Red trace (DT response), blue trace (mass response).

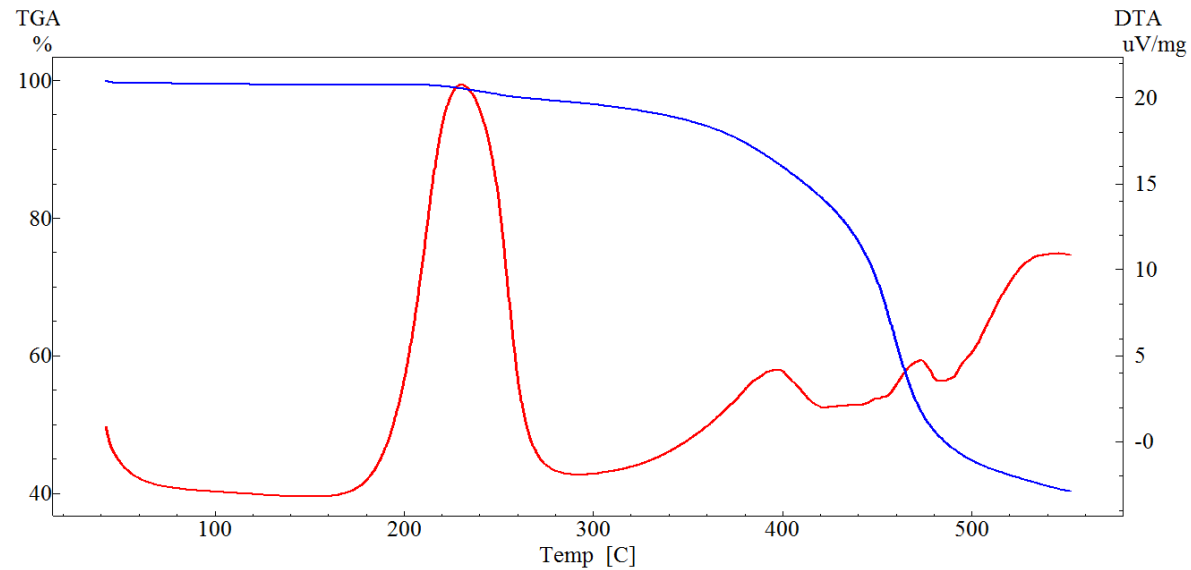


Figure S 12: TG-DTA of MSO₂Me-79 . Red trace (DT response), blue trace (mass response).

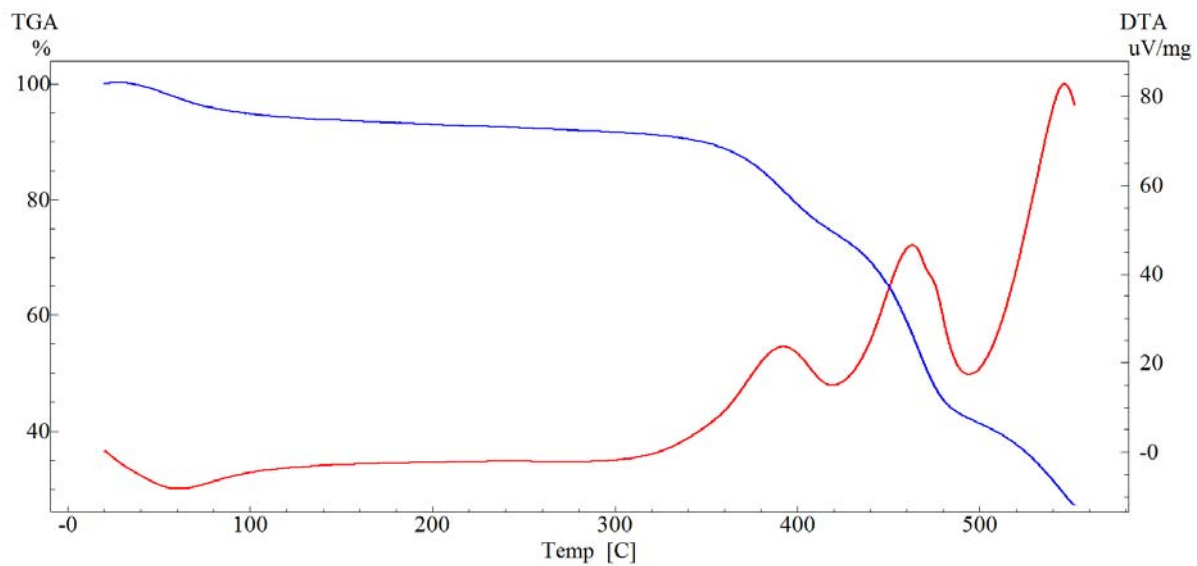


Figure S 13: TG-DTA of $\text{MSO}_2\text{Me}-100$. Red trace (DT response), blue trace (mass response).

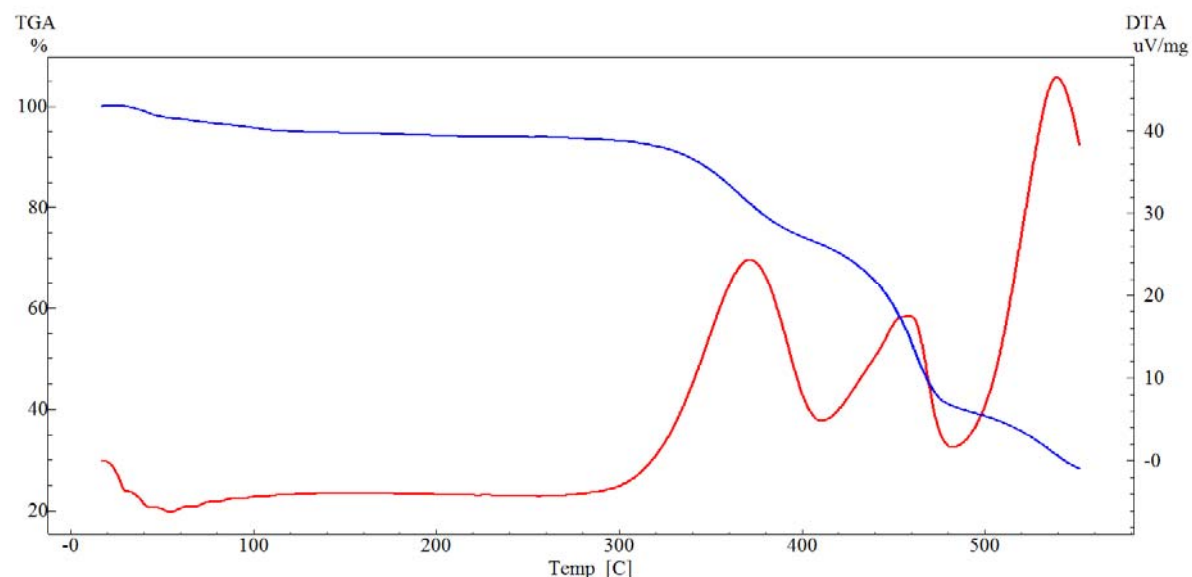


Figure S 14: TG-DTA of $\text{MSO}_2\text{Pr}-100$. Red trace (DT response), blue trace (mass response).

4. Gas Adsorption Analyses

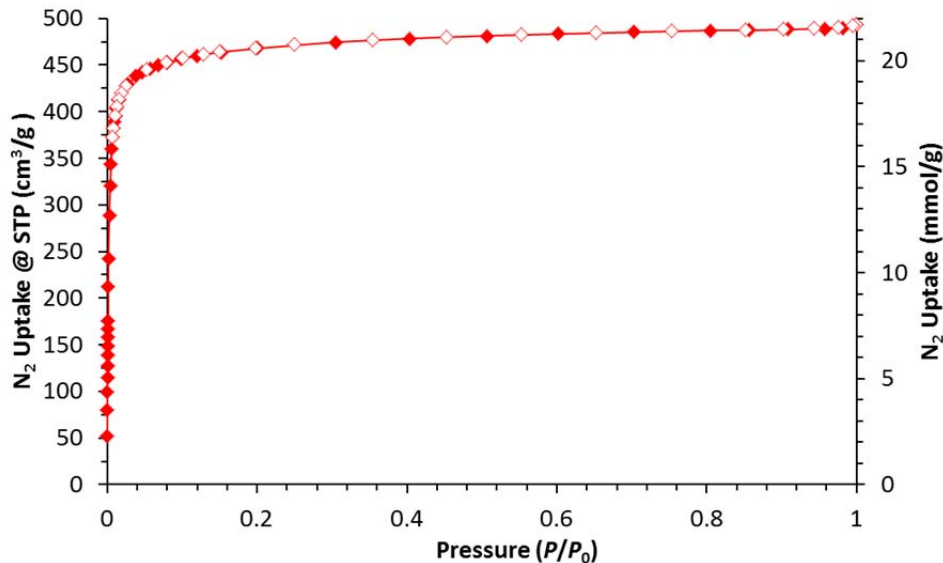


Figure S 15: N₂ gas adsorption isotherm at 77 K for MSO₂Me-15. Solid symbols indicate adsorption, empty symbols desorption. Line provided on the adsorption branch to guide the eye.

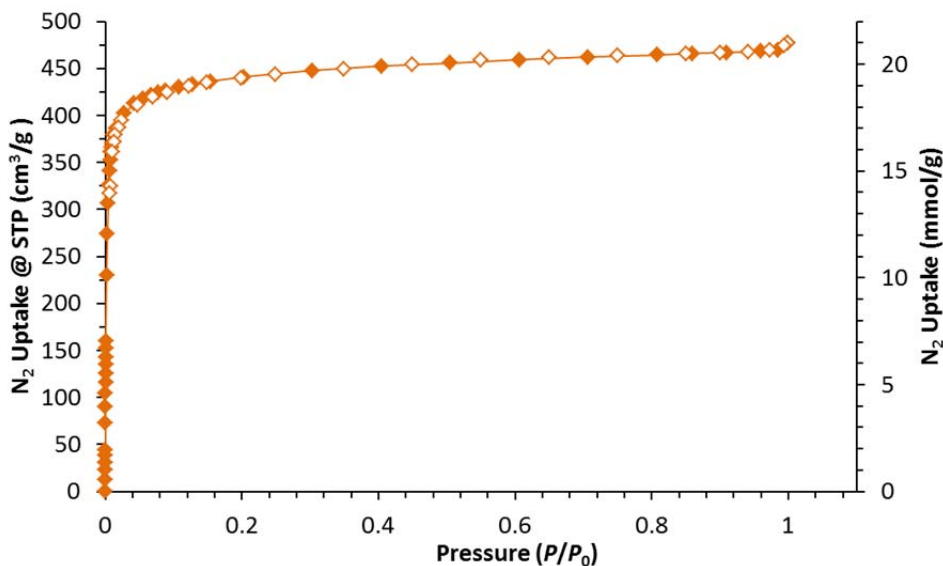


Figure S 16: N₂ gas adsorption isotherm at 77 K for MSO₂Me-36. Solid symbols indicate adsorption, empty symbols desorption. Line provided on the adsorption branch to guide the eye.

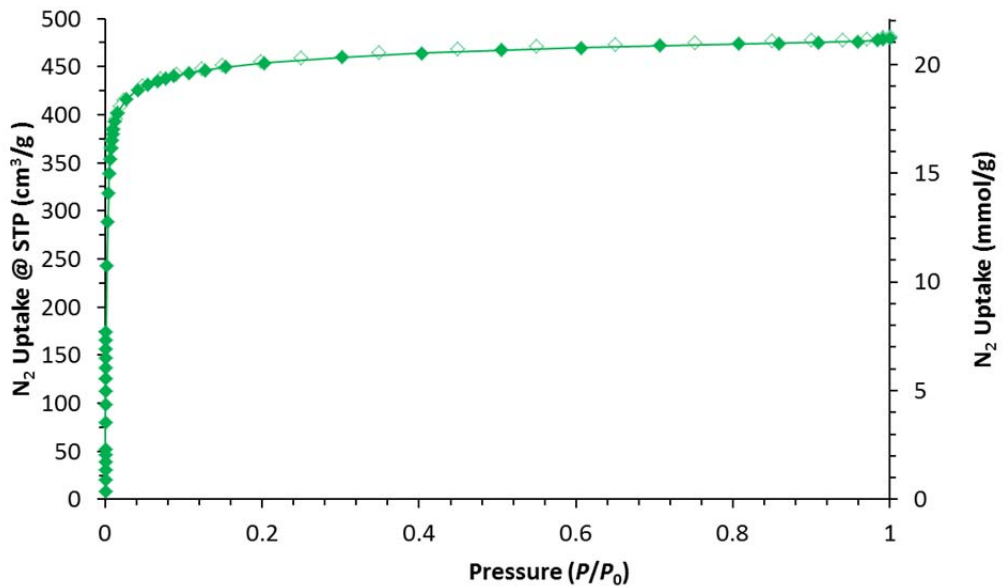


Figure S 17: N₂ gas adsorption isotherm at 77 K for MSO₂Me-64. Solid symbols indicate adsorption, empty symbols desorption. Line provided on the adsorption branch to guide the eye.

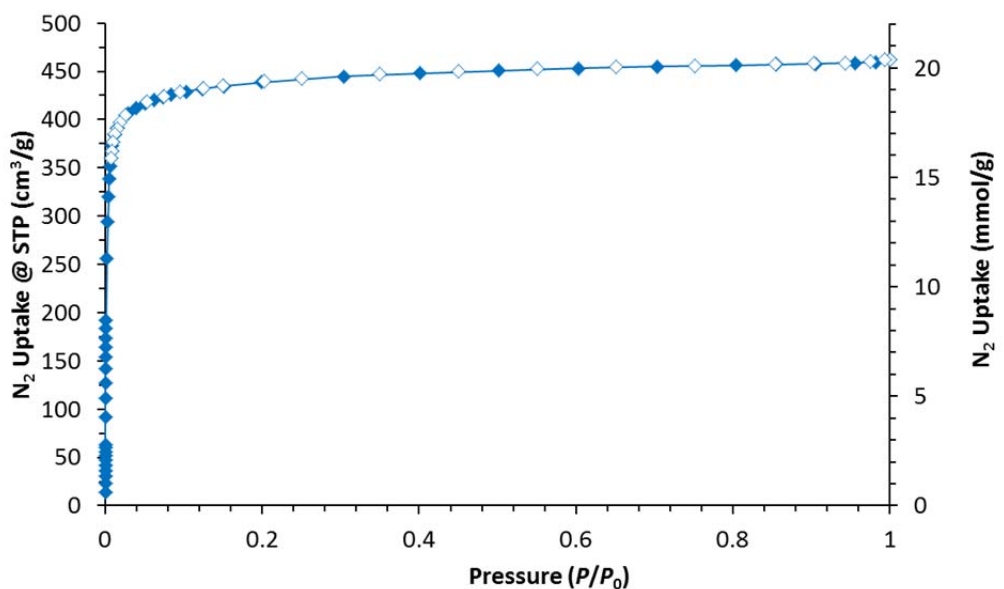


Figure S 18: N₂ gas adsorption isotherm at 77 K for MSO₂Me-79. Solid symbols indicate adsorption, empty symbols desorption. Line provided on the adsorption branch to guide the eye.

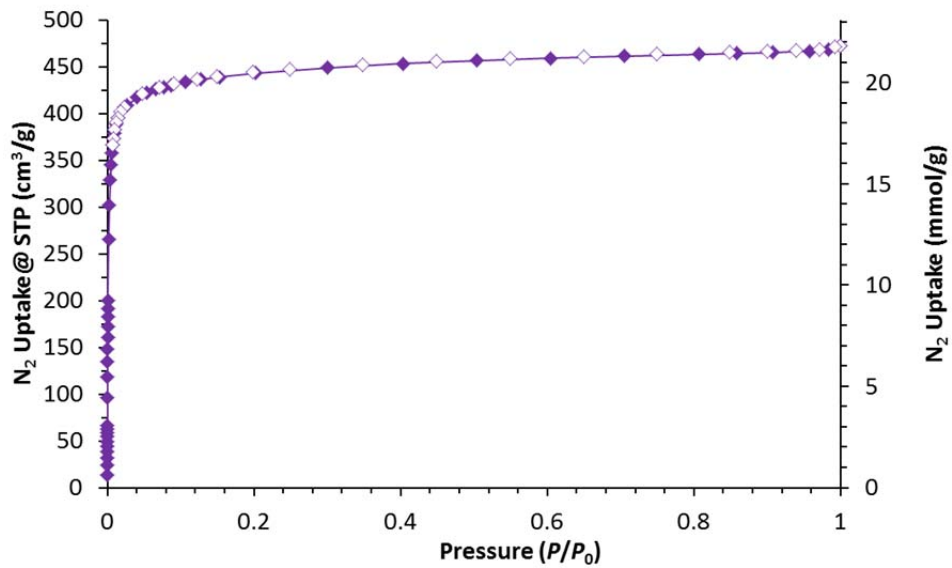


Figure S 19: N₂ gas adsorption isotherm at 77 K for MSO₂Me-100. Solid symbols indicate adsorption, empty symbols desorption. Line provided on the adsorption branch to guide the eye.

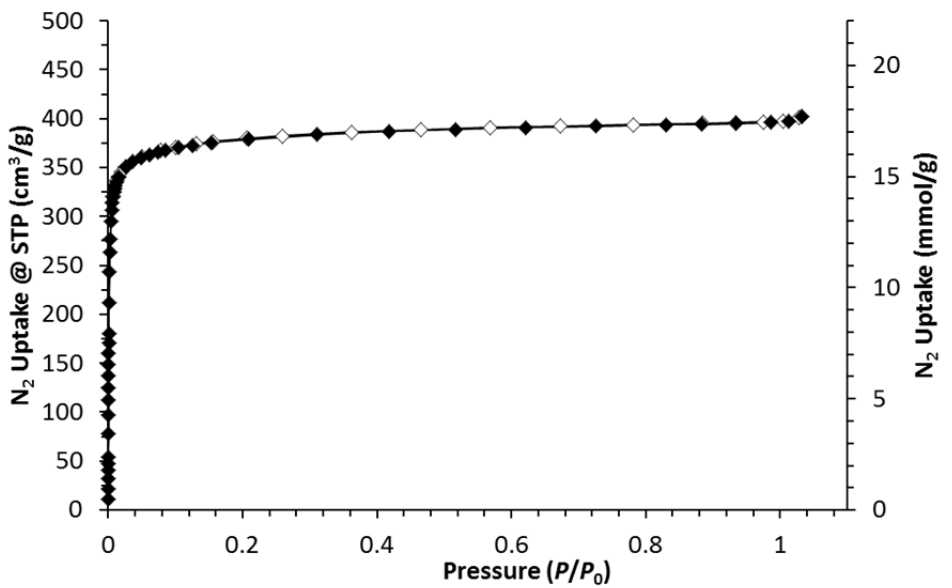


Figure S 20: N₂ gas adsorption isotherm at 77 K for MSO₂Pr-100. Solid symbols indicate adsorption, empty symbols desorption. Line provided on the adsorption branch to guide the eye.

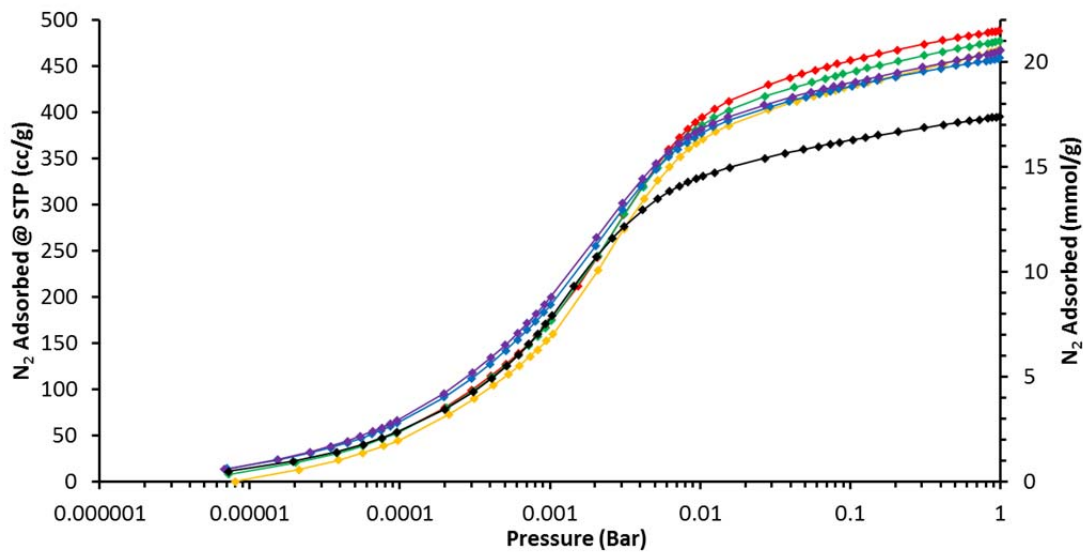


Figure S 21 N₂ gas adsorption isotherms at 77 K in log scale for MSO₂Me-15 (red), MSO₂Me-36 (orange), MSO₂Me-64 (green), MSO₂Me-79 (blue), MSO₂Me-100 (purple) and MSO₂Pr-100 (black). Lines provided on the adsorption branch as a guide for the eye.

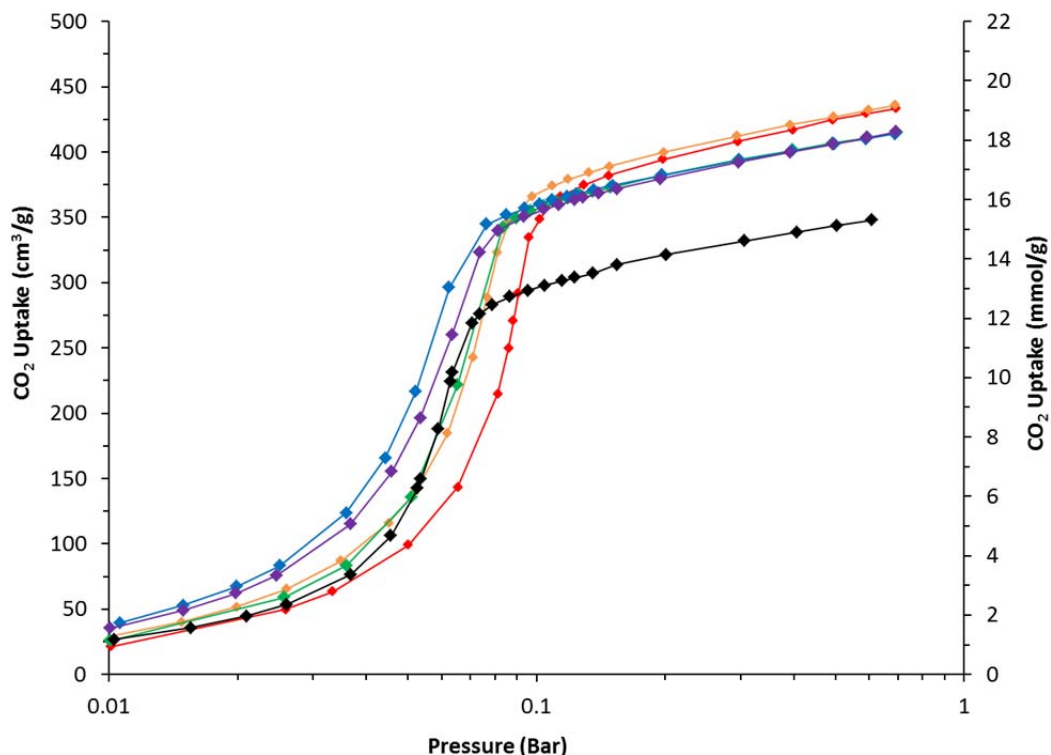


Figure S 22: CO₂ gas adsorption isotherms at 196 K in log scale for MSO₂Me-15 (red), MSO₂Me-36 (orange), MSO₂Me-64 (green), MSO₂Me-79 (blue), MSO₂Me-100 (purple) and MSO₂Pr-100 (black). Lines provided on the adsorption branch as a guide for the eye.

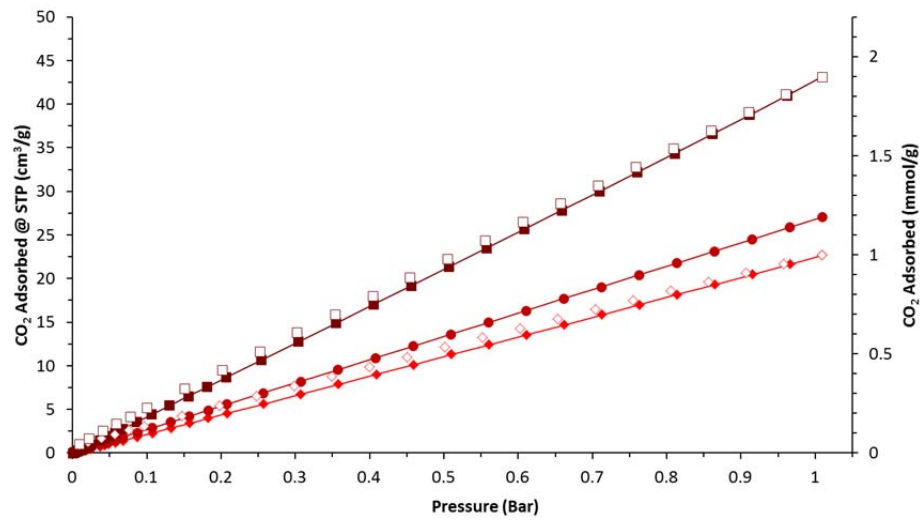


Figure S 23: CO₂ gas adsorption isotherms for MSO₂Me-15 at 273 K (squares), 288 K (circles) and 298 K (diamonds). Solid symbols indicate adsorption, empty symbols desorption. Lines provided on the adsorption branch to guide the eye.

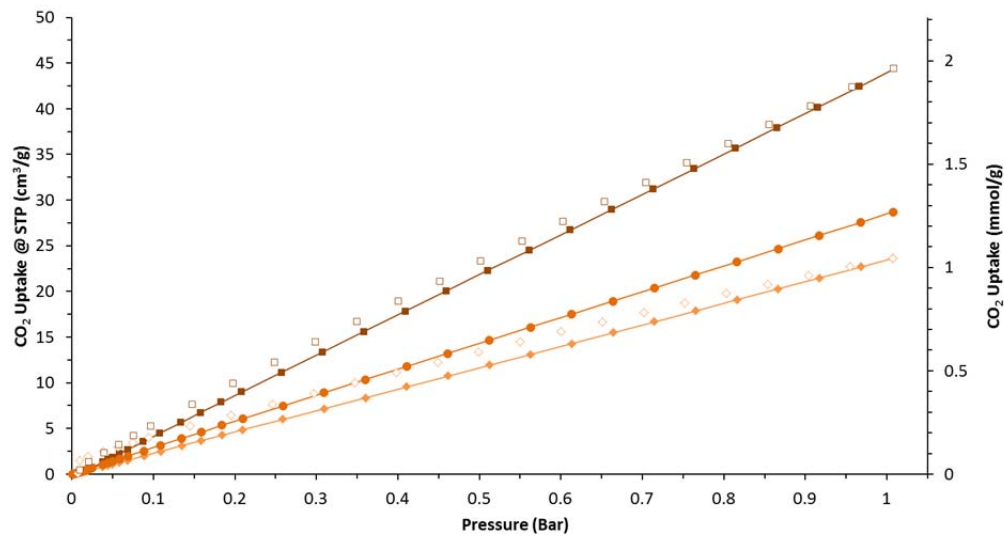


Figure S 24: CO₂ gas adsorption isotherms for MSO₂Me-36 at 273 K (squares), 288 K (circles) and 298 K (diamonds). Solid markers indicate adsorption, while empty markers indicate desorption. Lines are provided on the adsorption branch to guide the eye.

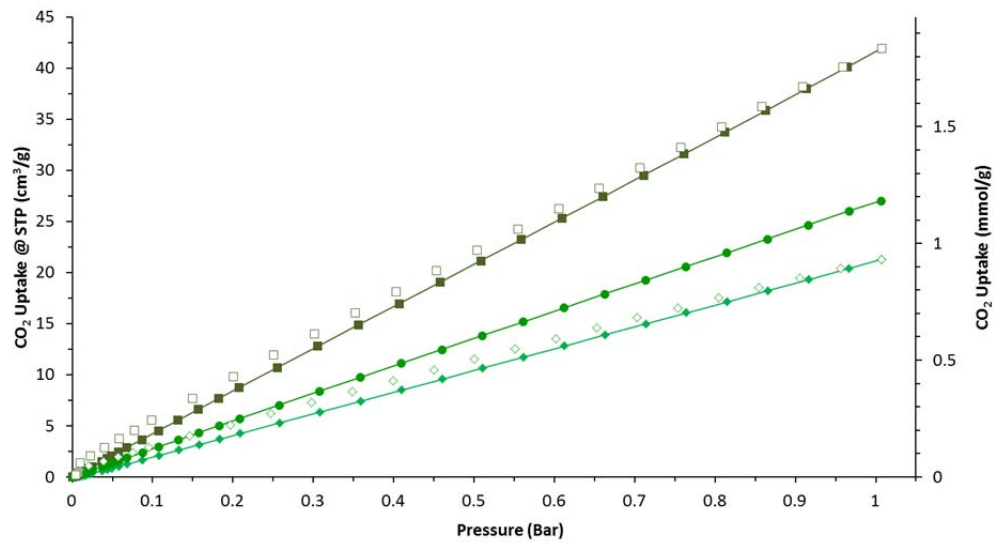


Figure S 25: CO₂ gas adsorption isotherms for MSO₂Me-64 at 273 K (squares), 288 K (circles) and 298 K (diamonds). Solid markers indicate adsorption, empty markers desorption. Lines provided on the adsorption branch to guide the eye.

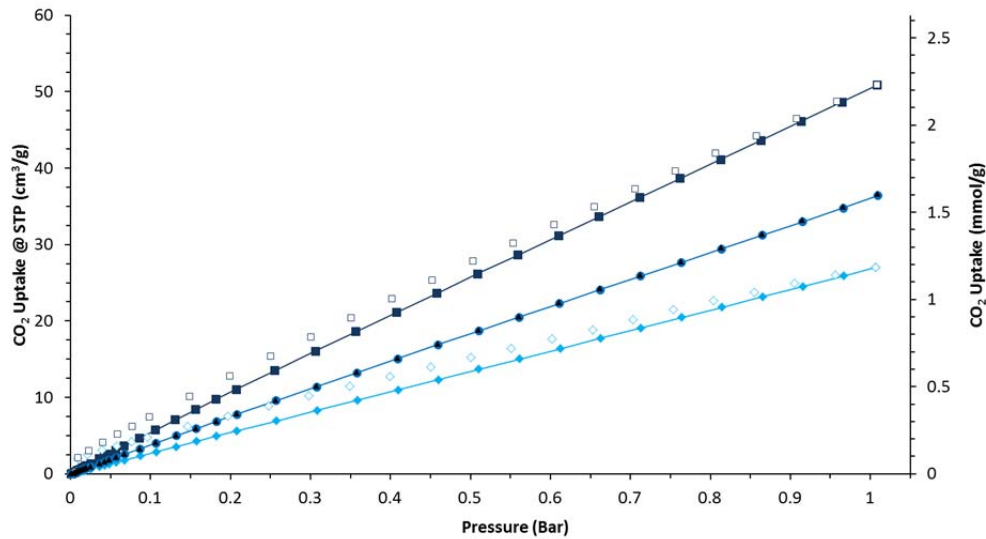


Figure S 26: CO₂ gas adsorption isotherms for MSO₂Me-79 at 273 K (squares), 288 K (circles) and 298 K (diamonds). Solid markers indicate adsorption, empty markers desorption. Lines provided on the adsorption branch to guide the eye.

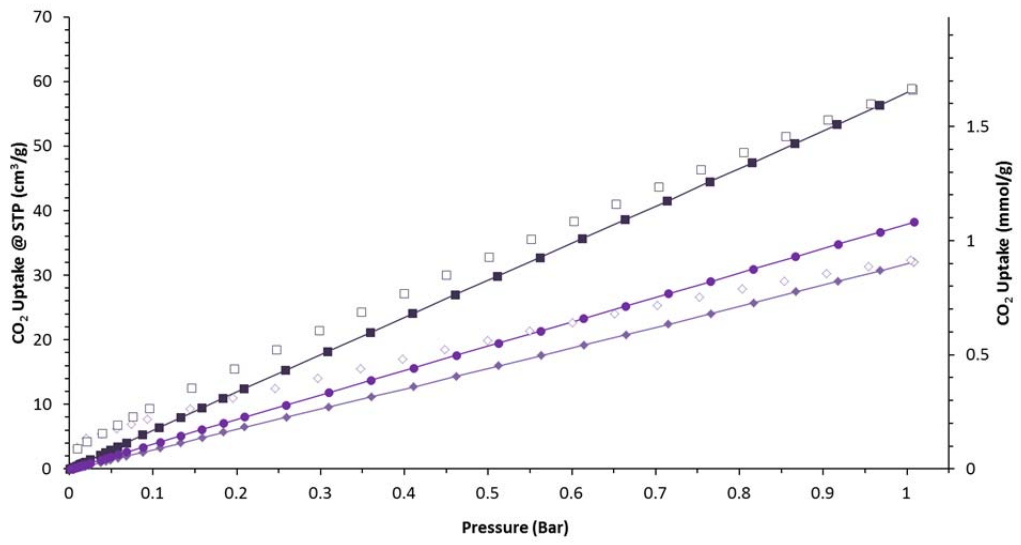


Figure S 27: CO₂ gas adsorption isotherms for MSO₂Me-100 at 273 K (squares), 288 K (circles) and 298 K (diamonds). Solid markers indicate adsorption, empty markers desorption. Lines provided on the adsorption branch to guide the eye.

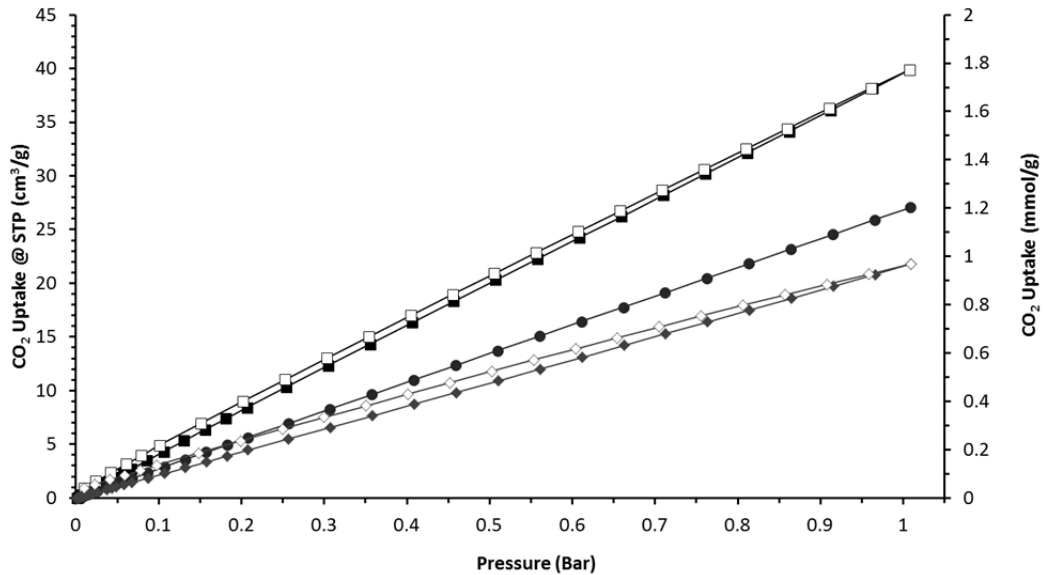


Figure S 28: CO₂ gas adsorption isotherms for MSO₂Pr-100 at 273 K (squares), 288 K (circles) and 298 K (diamonds). Solid markers indicate adsorption, empty markers desorption. Lines provided to guide the eye.

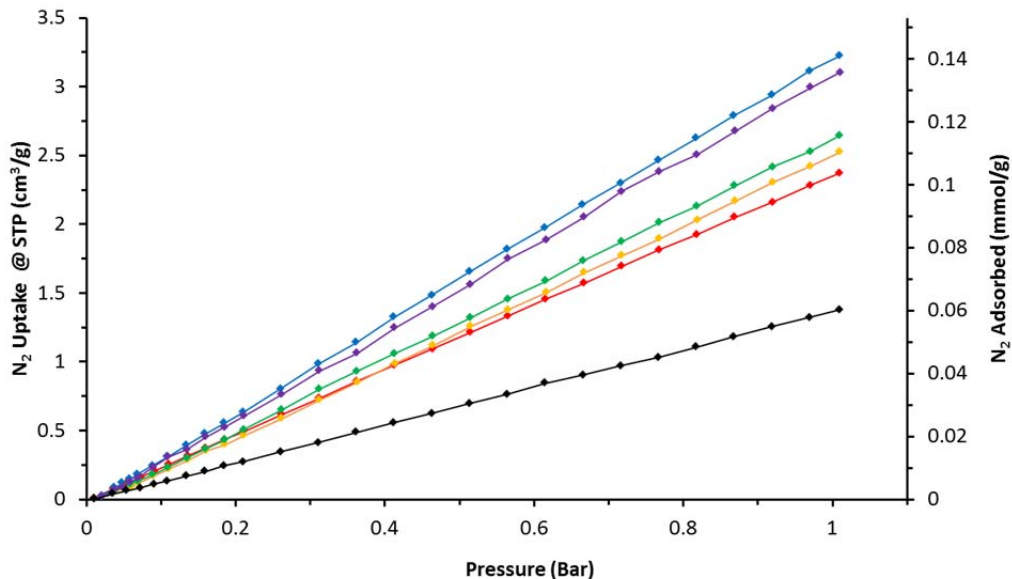


Figure S 29: N₂ gas adsorption isotherms at 298 K for MSO₂Me-15 (red), MSO₂Me-36 (orange), MSO₂Me-64 (green), MSO₂Me-79 (blue), MSO₂Me-100 (purple). Lines provided as a guide for the eye.

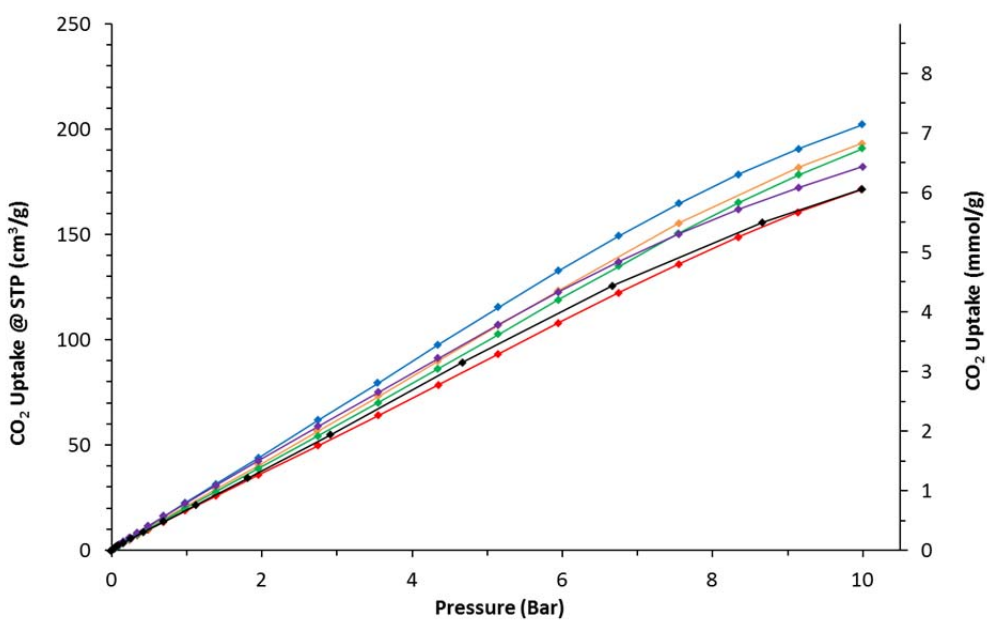


Figure S 30: CO₂ gas adsorption isotherms up to 10 bar at 298 K for MSO₂Me-15 (red), MSO₂Me-36 (orange), MSO₂Me-64 (green), MSO₂Me-79 (blue), MSO₂Me-100 (purple) and MSO₂Pr-100 (black).

5. Analyses Post Water Vapor Sorption

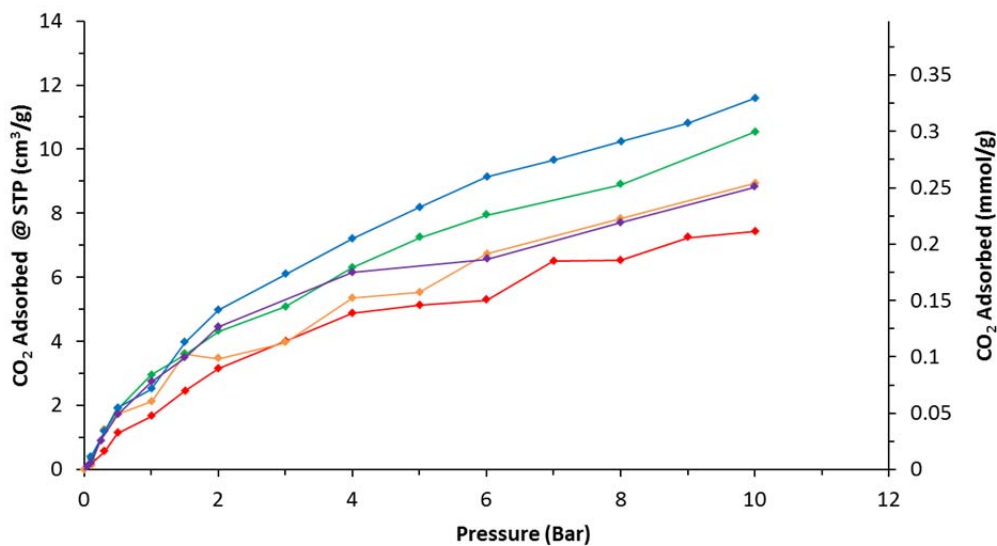


Figure S 31: CO₂ gas adsorption isotherms at 298 K after water sorption experiments for MSO₂Me-15 (red), MSO₂Me-36 (orange), MSO₂Me-64 (green), MSO₂Me-79 (blue), MSO₂Me-100 (purple)

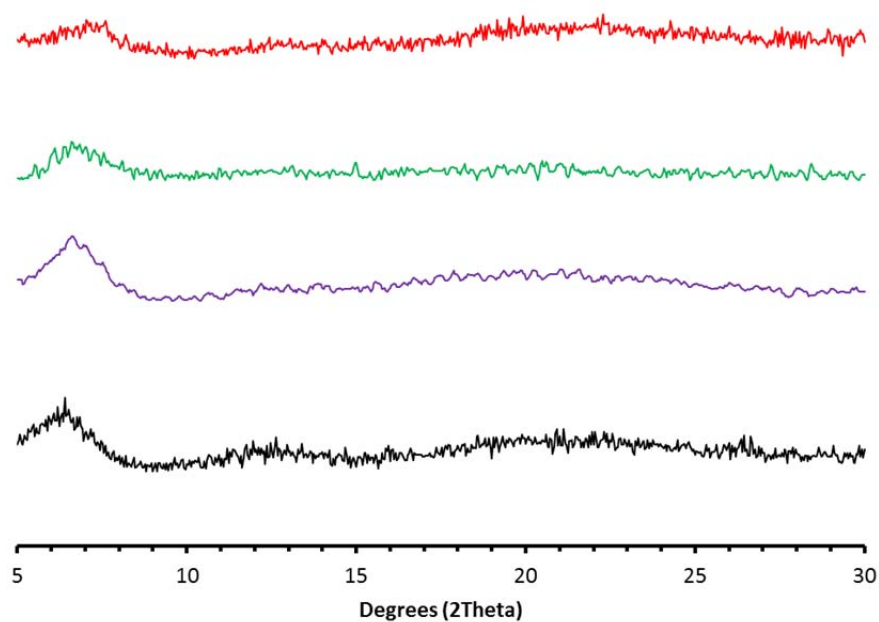


Figure S 32: PXRD patterns (post water isotherms) of MSO₂Me-15 (red), MSO₂Me-64 (green), MSO₂Me-100 (purple) and MSO₂Pr-100 (black).

6. Multi-Point Brunauer–Emmett–Teller Analyses

BET summary for MSO ₂ Me-15		
Slope	1.842	
Intercept	2.015e-03	
Correlation coefficient, r	0.999988	
C constant	915.053	
Surface Area	1888.418 m ² /g	
Relative Pressure	Volume @ STP	1 / [W((Po/P) - 1)]
8.05E-03	382.5912	1.70E-02
9.01E-03	389.6857	1.87E-02
9.99E-03	395.3278	2.04E-02
1.20E-02	403.9501	2.41E-02
1.50E-02	412.7747	2.96E-02
2.73E-02	430.339	5.22E-02
3.82E-02	438.3285	7.25E-02

BET summary for MSO ₂ Me-36		
Slope	1.975	
Intercept	2.02E-03	
Correlation coefficient, r	0.999991	
C constant	979.198	
Surface Area	1761.566 m ² /g	
Relative Pressure	Volume @ STP	1 / [W((Po/P) - 1)]
8.12E-03	360.7788	1.82E-02
9.09E-03	366.3686	2.00E-02
1.00E-02	370.7683	2.19E-02
1.21E-02	379.2738	2.59E-02
1.50E-02	386.0313	3.16E-02
2.75E-02	402.8491	5.62E-02
4.23E-02	412.5258	8.58E-02

BET summary for MSO ₂ Me-64		
Slope	1.904	
Intercept	1.86E-03	
Correlation coefficient, r	0.999986	
C constant	1026.815	
Surface Area	1827.641 m ² /g	
Relative Pressure	Volume @ STP	1 / [W((Po/P) - 1)]
8.08E-03	3.75E+02	1.74E-02
9.07E-03	3.81E+02	1.92E-02
1.00E-02	3.86E+02	2.09E-02
1.20E-02	3.95E+02	2.47E-02
1.51E-02	4.03E+02	3.05E-02
2.63E-02	4.18E+02	5.18E-02
4.09E-02	4.27E+02	7.99E-02

BET summary for MSO ₂ Me-79		
Slope	1.974	
Intercept	1.67E-03	
Correlation coefficient, r	0.999991	
C constant	1180.786	
Surface Area	1763.139 m ² /g	
Relative Pressure	Volume @ STP	1 / [W((Po/P) - 1)]
8.06E-03	367.6226	1.77E-02
9.05E-03	373.0102	1.96E-02
1.00E-02	377.1231	2.15E-02
1.21E-02	384.4763	2.54E-02
1.52E-02	391.3367	3.16E-02
2.90E-02	406.4924	5.88E-02
3.91E-02	412.3682	7.89E-02

BET summary for MSO ₂ Me-100		
Slope	1.959	
Intercept	1.53E-03	
Correlation coefficient, r	0.999991	
C constant	1277.867	
Surface Area	1776.293 m ² /g	
Relative Pressure	Volume @ STP	1 / [W((Po/P) - 1)]
8.12E-03	373.4879	1.75E-02
9.11E-03	378.5097	1.94E-02
1.00E-02	382.3198	2.12E-02
1.20E-02	388.5829	2.49E-02
1.51E-02	395.3855	3.10E-02
2.62E-02	408.4346	5.28E-02
4.06E-02	417.095	8.11E-02

BET summary for MSO ₂ Pr-100		
Slope	2.298	
Intercept	1.368e-03	
Correlation coefficient, r	0.999990	
C constant	1680.238	
Surface Area	1514.712 m ² /g	
Relative Pressure	Volume @	1 / [W((Po/P) - 1)]
9.07E-03	328.5264	2.23E-02
1.00E-02	331.405	2.44E-02
1.20E-02	334.9799	2.90E-02
1.52E-02	340.453	3.62E-02
2.59E-02	350.6017	6.07E-02
3.54E-02	355.7703	8.25E-02
4.70E-02	360.1145	1.10E-01

7. Fitting Parameters for IAST calculations

The IAST calculation was carried out using Pyiast.¹ The Henry model was used to fit the isotherms, which are linear at 298 K. The Henry coefficients for each isotherm are listed below together with the R² value indicating the quality of the fit.

MSO₂Me-15	Component	Henry Coefficient	Adj. R-Square	Standard Error
	CO ₂	0.9788	0.99981	0.00165
	N ₂	0.10361	0.99994	9.52444E-5

MSO₂Me-36	Component	Henry Coefficient	Adj. R-Square	Standard Error
	CO ₂	1.02788	0.99992	0.0011
	N ₂	0.10863	0.99799	5.89721E-4

MSO₂Me-64	Component	Henry Coefficient	Adj. R-Square	Standard Error
	CO ₂	0.92237	0.99962	0.00219
	N ₂	0.11457	0.99878	4.80334E-4

MSO₂Me-79	Component	Henry Coefficient	Adj. R-Square	Standard Error
	CO ₂	1.1792	0.99998	5.81835E-4
	N ₂	0.14094	0.99942	4.16062E-4

MSO₂Me-100	Component	Henry Coefficient	Adj. R-Square	Standard Error
	CO ₂	1.38717	0.99964	0.00312
	N ₂	0.13558	0.99912	4.81521E-4

MSO₂Pr-100	Component	Henry Coefficient	Adj. R-Square	Standard Error
	CO ₂	0.94516	0.99997	5.87551E-4
	N ₂	0.05971	0.99959	1.44825E-4

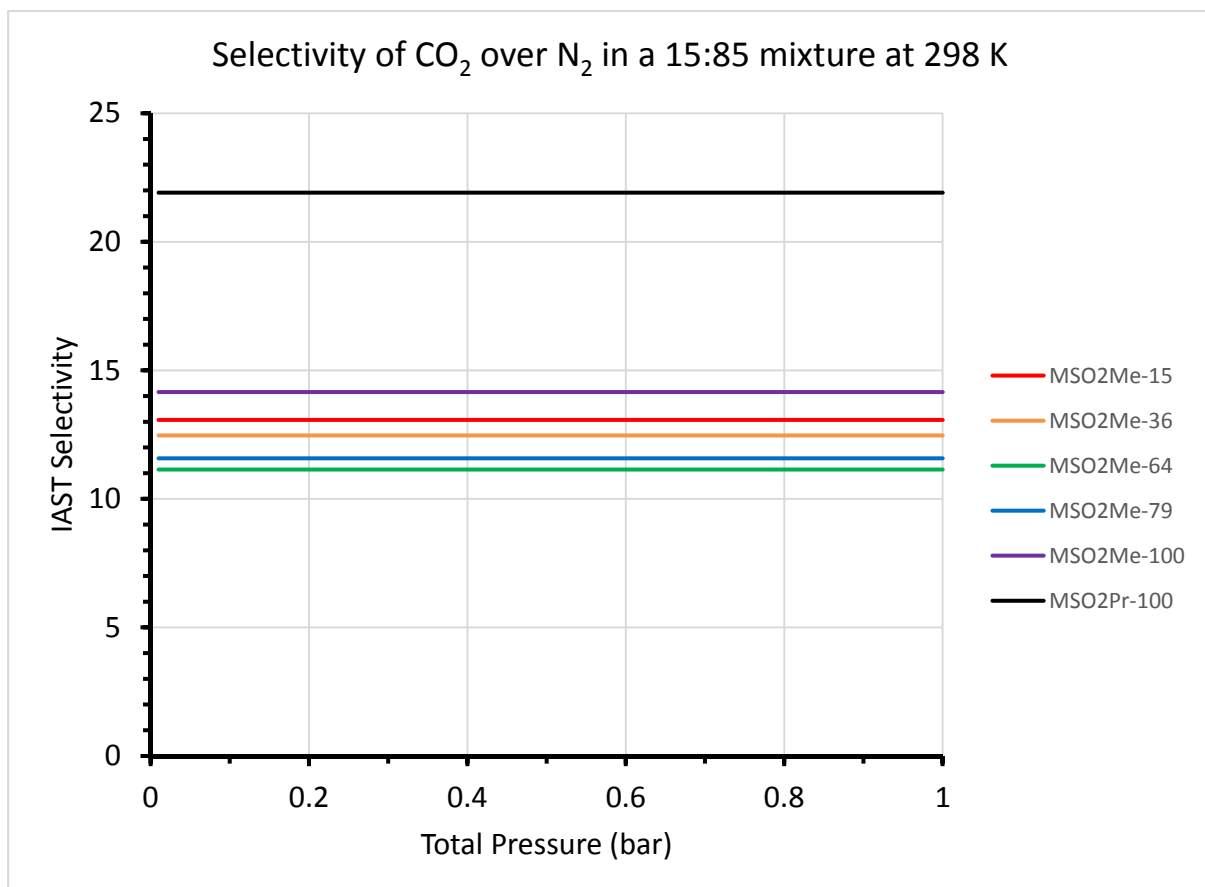


Figure S 33 IAST Selectivity plot of MSO₂Me-15 (red), MSO₂Me-36 (orange), MSO₂Me-64 (green), MSO₂Me-79 (blue), MSO₂Me-100 (purple) and MSO₂Pr-100 (black).

References:

1. Simon, C. M.; Smit, B.; Haranczyk, M. *Comput. Phys. Commun.* **2016**, *200*, 364-380.